Dual Ligand Insertion in gB and gD of Oncolytic Herpes Simplex Viruses for Retargeting to a Producer Vero Cell Line and to Cancer Cells

Previous version JVI01224-17

Dual ligand insertion in gB and in gD of oncolytic HSVs for the retargeting to a producer Vero cell line and to cancer cells.

Biljana Petrovic[1*], Valerio Leoni[1*], Valentina Gatta[1], Anna Zaghini[2], Andrea Vannini[1], Gabriella Campadelli-Fiume[1]

[1]Department of Experimental, Diagnostic and Specialty Medicine, [2]Department of Veterinary Medical Sciences ,University of Bologna, Bologna, Italy.

Running Head: Dual gB gD retargeting of oncolytic HSVs

Address correspondence to
Gabriella Campadelli-Fiume
Department of Experimental, Diagnostic and Specialty Medicine
University of Bologna
Via San Giacomo, 12
40126 Bologna, Italy
tel +39 051 2094733/34
FAX +39 051 2094735
email gabriella.campadelli@unibo.it

* contributed equally to this work

KEYWORDS. HER2, HSV, retargeting, gD, gB, Vero, oncolytic virus

ABSTRACT

Oncolytic viruses gain cancer specificity in several ways. Like the majority of viruses, they grow better in cancer cells which are defective in mounting the host response to viruses. Often they are attenuated by deletion or mutation of virulence genes which counteract the host response, or are naturally occurring oncolytic mutants. In contrast, retargeted viruses are not attenuated or deleted; their cancer-specificity rests on a modified, specific tropism for cancer receptors. For herpes simplex virus (HSV)-based oncolytics, the detargeting-retargeting strategies employed so far were based on genetic modifications of gD. Recently, we showed that even gH or gB can serve as retargeting tools. To enable the growth of retargeted HSVs in cells that can be used for clinical grade virus production, a double retargeting strategy has been developed. Here we show that several sites in the N-terminus of gB are suitable to harbour the 20 aa long GCN4 peptide, which readdresses HSV tropism to Vero cells expressing the artificial GCN4 receptor, and thus enables virus cultivation in the producer non-cancer Vero-GCN4R cell line. The gB modifications can be combined with a minimal detargeting modification in gD, consisting in the deletion of two residues, aa 30 and 38, and replacement of aa 38 with the scFv to HER2, for retargeting to the cancer receptor. The panel of recombinants was analysed comparatively in terms of virus growth, cell-to-cell spread, cytotoxicity, *in vivo* anti-tumor efficacy to define the best double retargeting strategy.

IMPORTANCE

There is increasing interest in oncolytic viruses, following FDA and EMA approval of HSV Oncovex$^{GM\text{-}CSF}$, and, mainly, because they greatly boost the immune response to the tumor and can be combined with immunotherapeutic agents, particularly checkpoint inhibitors. A strategy to gain cancer specificity and avoid virus attenuation is to retarget the virus tropism to cancer-specific receptors of choice. Cultivation of fully retargeted viruses is challenging, since they require cells that express the cancer receptor. We devised a strategy for their cultivation in producer non-cancer Vero cell derivative. Here, we developed a double retargeting strategy, based on insertion of one

ligand in gB for retargeting to Vero cell derivative, and of anti-HER2 ligand in gD for cancer retargeting. These modifications were combined with a minimally-destructive detargeting strategy. Current and accompanying study teach the clinical-grade cultivation of retargeted oncolytic HSVs, and promote their translation to the clinic.

INTRODUCTION

Oncolytic viruses constitute a recent class of anti-cancer therapeutics, which can be armed with cytokines, and can be administered in combination with checkpoint inhibitors (1-8). Oncolytic viruses may be wt viruses, natural mutants, animal viruses with tropism for human cells, or genetically engineered viruses. They share the ability to infect, replicate in, and kill cancer cells. Numerous oncolytic viruses from different viral families are being evaluated in clinical trials (9-12). The oncolytic virus originally named Oncovex^{GM-CSF} has been approved by FDA and EMA against metastatic melanoma (13, 14).

A key requirement for oncolytic viruses is cancer specificity. For a number of viruses, the specificity rests on a higher ability to replicate in cancers cells, which are usually defective in some branches of the innate response (2, 15). Other viruses, exemplified by Oncovex^{GM-CSF}, were engineered so as to attenuate them, i.e. to delete virulence genes which counteract the host response (13, 16). Hence, they are defective in replication in non-cancers cells, and replicate in cancer cells to varying degrees. The most highly attenuated viruses may exhibit limited replication even in cancer cells (17).

An alternative strategy to attenuation is the tropism retargeting, whereby the viral tropism is retargeted to cancer-specific receptors of choice, and detargeted from natural receptors; the viruses are otherwise wt, i.e. non-attenuated (18-22). In our laboratory we selected as the target receptor HER2 (human epidermal growth factor receptor 2) (20, 22-27), a member of the EGFR (epidermal growth factor receptor) family of receptors, present in a subset of breast, ovary, stomach and lung cancers. The patients carrying HER2-positive tumors are treated with the anti-HER2 humanized antibodies trastuzumab and/or pertuzumab (28, 29). However, a fraction of patients does not respond (30). Those who respond, develop resistance, frequently within a year of treatment, with mechanisms which do not involve the loss of HER2 ectodomain. In our earlier studies the tropism retargeting has been achieved by deletion of gD sequences critical for interaction with the gD natural receptors HVEM and nectin1 (detargeting), either aa 6-38, or aa 61-218, and their

replacement with a scFv to HER2 derived from trastuzumab (20, 22, 31). These recombinants, named R-LM113 and R-LM249, exhibit strong oncolytic/therapeutic activity in nude mice xenotransplanted with human HER2-positive ovary or breast cancers, including metastatic cancers and a glioblastoma model (23-26).

The HER2-retargeted oncolytic HSVs employed so far in preclinical studies were cultivated in cancers cells, a procedure which may not be approvable for the growth of clinical grade viruses. Recently, we have developed a strategy, based on double retargeting, for cultivation of retargeted oHSVs in non-cancer cells (32). Briefly, gD carries the scFv to HER2 in place of aa 6-38, for cancer retargeting, while gH carries the 20 aa long GCN4 peptide, derived from the yeast transcription factor (recombinant R-213). The GCN4 peptide enabled infection of Vero cells expressing an artificial receptor, named GCN4R, made of a scFv to GCN4 (33) fused to domain II, III, TM and C tail of nectin1 (32). Subsequently, we showed that also gB can be a tool for retargeting and accepts the insertion of the scFv to HER2 at a specific position, between aa 43-44 (34). The choice of the Vero cells as recipient of GCN4R rested on the notion that wt Vero cells have been approved by FDA for the clinical grade preparations of Oncovex^{GM-CSF} (commercial name Imlygic), the derivative named Vero-His (35) is approved for clinical grade preparations of oncolytic Measles viruses, and, more generally, wt Vero are approved for growth of a number human vaccines.

The aims of this work were twofold. First, to ascertain whether the simultaneous retargeting to two targets – GCN4R and HER2 - could be achieved by insertion of the GCN4 peptide in gB and detargeting plus HER2-retargeting *via* gD. Second, to develop a novel, minimally invasive strategy for detargeting gD from its natural receptors. We report that gB can accept the GCN4 retargeting peptide at several positions for *in vitro* cultivation in non-cancer cells; one such modification was combined with a gD detargeting strategy based on the deletion of two single amino acids (residues 30 and 38), and substitution of aa 38 with the scFv to HER2 for retargeting to the cancer receptor.

RESULTS

Insertion of ligands in gB and in gD for the simultaneous retargeting to two different targets. We generated four recombinants, R-313, R-315, R-317, and R-319 carrying the GCN4 peptide in gB at one of the following sites, between aa 43-44, 81-82, 76-77, 95-96, and carrying the scFv to HER2 in gD, in place of aa 6-38 (Fig. 1 and Table 1). The tropism of the recombinants was evaluated in the HER2-positive SK-OV-3 cancer cells, in the Vero-GCN4R, in wt-Vero, and in derivatives of the receptor-negative J cells, transgenically expressing a single receptor, e.g. HER2, nectin1, or HVEM (20, 36). R-LM113, retargeted to HER2 but not to GCN4R was included as control. Fig. 2 A-D shows that the recombinants R-313, R-315, R-317, and R-319 viruses were retargeted to GCN4R, as indicated by the ability to infect Vero-GCN4R cells, in the presence of the anti-HER2 MAb trastuzumab. All recombinants were retargeted to HER2, as indicated by ability to infect J-HER2 and SK-OV-3 cells in a trastuzumab-dependent fashion. This property is shared with R-LM113 (Fig. 2 E). Consistent with the Δ6-38 in gD and replacement of the deleted sequences with the scFv to HER2 (22), all recombinants failed to infect J-HVEM and J-nectin1 cells, i.e. they were detargeted from natural gD receptors. They infected the wt-Vero cells in a trastuzumab-inhibited fashion, very likely through the simian orthologue of HER2. Indeed, the whole genome sequence of Vero cell is incomplete, and, so far, there is no documentation of a HER2 homologue in this cell line. Nonetheless, Vero cells were isolated from an Africa Green Monkey (Chlorocebus sp.), and the sequence of the Chlorocebus genome contains the HER2 homologue (Chlorocebus sabaeus; REFSEQ: XM_008012845.1) with 98% identity with the human HER2. We conclude from these results that the four insertion sites tested were all suitable for insertion in that the generated recombinants were viable, implying that gB carried out the fusogenic function. More importantly, the inserted GCN4 peptide mediated infection through the GCN4R, i.e. it was suitably located in gB not only to prevent any detrimental effect on gB function, but also to contribute to its entry function, i.e. to the GCN4R-dependent infection and consequent gB activation. The insertions in gB could be combined with the retargeting to HER2 through deletion/scFv insertion in gD.

Novel gD detargeting strategy. In the four recombinants described above the detargeting from the natural gD receptors was achieved by deletion of the 6-38 region, which contains residues critical for interaction with HVEM and nectin1, and its replacement with the scFv to HER2. Here we asked whether the detargeting could be achieved by a less invasive strategy. We deleted aa 30 and 38, and replaced aa 38 with the scFv to HER2. The modification in gB was the same as the one present in R-313, i.e. the insertion of the GCN4 peptide between aa 43 and 44. The resulting recombinant was named R-321 (for a schematic drawing of the genotype, see Fig. 1 B, and Table 1). Its tropism is shown in Fig. 2 F. R-321 failed to infect J-nectin1 and J-HVEM cells. Thus, the simple deletion of the two residues in gD was sufficient to detarget the virus tropism from the two natural gD receptors. R-321 was retargeted to HER2 (trastuzumab-dependent infection of SK-OV-3 and J-HER2 cells), hence the insertion of the scFv in place of aa 38 led to retargeting. The retargeting v*ia* the GCN4 insertion in gB was not modified relative to that seen in R-313, as expected.

Replication and cell-to-cell spread of the double retargeted recombinants. We measured the growth capacity of the recombinants in SK-OV-3 and in Vero-GCN4R cells. Fig. 3 A and B shows results of a typical experiment. The three of the recombinants, R-315, R-317, and R-321 could not be differentiated one from the other, and exhibited a high replication capacity in SK-OV-3 cells at 48 h. They replicated about as well as the R-LM113, which only carries the aa 6-38 deletion and the scFv insertion in place of the deleted sequence, and no modification in gB. The recombinant replicated as efficiently as R-LM5, which carries no deletion and no retargeting moiety at all (22). With respect to R-LM113, we note that this recombinant replicated for one passage in wt-Vero cells, and its Vero-GCN4R derivative; however, numerous efforts to passage serially R-LM113 in these cells were unsuccessful, and did not yield any progeny. Whether the defect in serial passages depends on low density of the receptor, low affinity-avidity between simian HER2 and the scFv to human HER2 inserted in R-LM113, or other, remains to be investigated. In both cells, R-315, R-317 and R-321 replicated better that R-313 and R-319. In Vero-GCN4R the yield of all

recombinants was about half-to-one log lower than that in SK-OV-3 cells, in agreement with earlier observations on gH-retargeted recombinants (32). We conclude from these results that not all the insertion sites in gB are equivalent with respect to virus infection/replication ability.

Fig. 3 A and B also shows the replication of R-87, for comparison. R-87 is described in accompanying paper (37). It carries the same ligands as the recombinants described in this paper, i.e. the scFv to HER2 and the GCN4 peptide. However, both ligands are engineered in gD. In particular, the scFv to HER2 replaces aa 35-39, and the GCN4 is inserted between aa 24 and 25 (see, Fig. 1 C and Table 1). Fig. 3 A and B show that the yields of R-87 were very similar to those of the best performing R-315, R-317 and R-321, notwithstanding the differences in the design of the two sets of viruses. A comparison was made also to R-213, a recombinant which carries the GCN4 peptide in gH, between aa 23-24, and the same modifications in gD as R-313, R-315, R-317 and R-319 (see Fig. 1 B) (32). Overall, R-213 replicated to similar yields as the recombinants generated in this study in SK-OV-3 cells at 48 h, and at somewhat lower yield in Vero-GCN4R cells (Fig. 3). Next, we measured the cell-to-cell spread. Typical examples of plaques are shown in Fig. 4 A, and average plaque sizes are quantified in Fig. 4 B. All recombinants produced plaques medium-to-large in size in Vero-GCN4R cells, and medium in size in SK-OV-3 cells. Importantly, all recombinants were more effective in cell-to-cell spread in Vero-GCN4R cells than R-LM113 (Fig. 4 B). With respect to the relative number of plaques in Vero-GCN4R and in SK-OV-3 cells, there was no significant difference among R-313, R.315, R-317 and R-319 (Fig. 4 C). There was a clear advantage of the recombinants over R-LM113 in Vero- GCN4R cells, as expected. With respect to plaque number, but not to plaque size, the recombinant R-213 which carries the GCN4 in gH (32) was superior in Vero-GCN4R (Fig. 4 C). Thus, although the gH recombinant needs further improvements, it shows interesting properties worth to be explored.

Cytotoxicity induced by the double-retargeted recombinants. An important property for any candidate oncolytic virus is the ability to kill cells. Hence, it was critical to ascertain whether the GCN4-retargeting *via* gB affected the virus-induced cytotoxicity. Monolayers of SK-OV-3 and

Vero-GCN4R were infected with the recombinants, with R-87 for comparison, and with R-LM5 and R-LM113 as controls. Cytotoxicity was measured by means of alamarBlue at the indicated days after infection. Fig. 5 shows that all recombinants exerted similar cytotoxic effects. The exception was R-LM113 in Vero-GCN4R cells, as expected.

Oncolytic efficacy of the double retargeted recombinant R-317 in immunocompetent mice. We selected R-317, one of the best performing double retargeted recombinants, to evaluate the oncolytic efficacy in immunocompetent mice. The animal model will be described elsewhere in details under different co-authorship (38). Essentially, it consists of the Lewis lung murine carcinoma 1 (LLC-1) cells made transgenic for human HER2 (hHER2-LLC-1). The cancer cells were implanted in a strain of the syngeneic C57BL6 mice, which are transgenic for, hence tolerant to hHER2. Three days after implantation of the tumor cells, R-317 was administered intratumorally (i.t.) at 3-4 days distance, with 1 x 10E8 PFU/each injection, for a total of 4 treatments. As a comparison we included in the experiment the prototypic R-LM113 and R-87 described in the accompanying paper (37). Fig. 6 A-C shows that the antitumor efficacy of R-317 was very similar to those of R-LM113 and of R-87. The tumor size at 28 d was significantly different from that in untreated mice (Fig. 6 D).

DISCUSSION

gB is a highly structured glycoprotein, little prone to accept insertions or mutations, except for the N-terminal region up to about aa 100. The N-terminal region is highly flexible and was disordered in gB post-fusion crystal structure (39-43). Previously, Potel et al. inserted the GFP moiety in gB at residues 43-44; the chimeric form of gB gave rise to a viable recombinant, indicating that the fusion-performing activity of gB had not been hampered (44). Gallagher et al. inserted fluorescent proteins in each of the three globular domains of gB. Only one third of the constructs were functional in the cell-cell fusion assay; in the functional constructs, the inserts were located either in the N-terminus, up to residue 100, or at residues 470 and 481 (45). A remarkable difference between those studies and the current one is that in the earlier studies the inserted fluorescent proteins were not employed as novel retargeting ligands. Hence, it was unknown whether retargeting could be achieved by ligand insertion at these sites. In a previous work, we inserted the scFv to HER2 in gB between aa 43-44; the viable recombinant indicated that this is an appropriate site for insertion of a retargeting ligand (34). Whether other insertion sites enabled the generation of viable recombinants, and whether the recombinants were retargeted was unknown. Recently we developed a double retargeting strategy for growth of clinical grade retargeted oncolytic HSVs. The strategy is based on the simultaneous retargeting to the HER2 cancer receptor (or other cancer targets of choice), and to the GCN4R present in the producer Vero cells (32). The aim of current work was to optimize two series of genetic modifications, i.e. ligand insertions in gB finalized to *in vitro* growth in non-cancer cells, and to define a novel, minimally-destructive strategy for detargeting from natural gD receptors and retargeting to cancer receptors. We generated a recombinant carrying the two series of modifications. The novel data to emerge are as follows.

gB can accept the insertion of the GCN4 retargeting peptide at various sites in the N-terminus. The investigated sites were not equivalent one to the other. Thus, the highest yields were achieved by R-315 and R-317, which harbour inserts at aa 81-82 or 76-77, respectively. The yields of these recombinants were very similar to that of R-LM113, which does not carry any modification

248 in gB, suggesting that the perturbations to gB induced by the GCN4 peptide at the 81-82 or 76-77
249 sites had a negligible effect. A decrease in virus yield was observed with R-313 and R-319, which
250 carry the GCN4 insert between aa 43 and 44, or between aa 95 and 96. The latter insertion site is
251 close to the downstream region which does not tolerate mutagenesis (42, 46). With respect to cell-
252 to-cell spread in SK-OV-3 cells, the recombinants R-313, R-315, R-317 and R-319 did not
253 significantly differ one from the other. R-319 exhibited the highest spread capacity in Vero-GCN4R
254 cells. Surprisingly, the recombinants performed somewhat better than the parental R-LM113, with
255 which they share the same gD modifications, hinting that the modifications to gB favour rather than
256 hamper cell-to-cell spread of the virus. All in all, it appears that the added ability to interact with a
257 gB receptor (in this case the GCN4R) adds to the cell-to-cell spread capacity of the recombinants,
258 without hampering the virus growth capacity. We note that mutagenesis of gH or gB at some sites
259 resulted in forms of the glycoproteins with enhanced cell-cell fusion activity, interpreted as a
260 promotion of gH or gB "activation" (19, 47-49). R-317, one of the best performing double
261 recombinants was also evaluated for *in vivo* anti-tumor efficacy, in an immunocompetent mouse
262 model. The model will be described elsewhere (38). It consists of the C56BL6 mice transgenic and
263 hence tolerant to human HER2 (hHER2), and the murine Lewis lung carcinoma 1 (LLC-1) cells
264 made transgenic for hHER2. As noted by several groups, the murine cells, including cancer cells
265 are scarcely permissive to HSV-1 (50, 51). The cells syngeneic with the C57BL6 mice are among
266 the most resistant. As a consequence, the model underestimates the efficacy of oncolytic HSVs. As
267 expected from the cell culture replication, the antitumor efficacy of R-317 was very similar to that
268 of R-LM113 and of R-87. Thus, the *in vitro* comparative properties are predictive of the *in vivo*
269 antitumor efficacy, and a double retargeted recombinant is as effective as the singly retargeted R-
270 LM113 virus.

271 Novel detargeting strategy. In earlier retargeted oncolytic HSVs, detargeting was a more
272 demanding task than the actual retargeting (18, 20, 52). The reason for that was that the actual
273 location of the nectin1 binding site in gD was not fully known. Taking advantage of the elucidation

of the co-crystal structure of nectin1-bound gD (53), here we designed a less invasive detargeting strategy (R-321). It consists of the deletion of two residues, aa 30 and aa 38, structurally involved in the interaction of gD with HVEM and nectin1, respectively (53-55). Our data show that the two single deletions and the replacement of aa 38 with scFv to HER2 were sufficient to detarget the HSV tropism from both natural receptors. Consistent with current data, the single mutagenesis of aa 38 was sufficient for nectin1 detargeting (21). It is worth comparing the growth properties of R-313 and R-321. The two recombinants share the same gB modifications, and differ in the portions of gD deleted for detargeting purposes. R-321 grew to about one log higher yield than R-313. Thus, decreasing the deleted portion of gD significantly rescued viral replication. Altogether, current study extends our notions on gB as a retargeting tool, and combines the retargeting *via* gB to novel detargeting strategy *via* gD.

In an accompanying paper, we show that double retargeting is feasible also by the simultaneous insertion of both the GCN4 peptide and the scFv in gD (37). Even in that case, the optimization can be achieved by a novel gD detargeting strategy. Results on R-87 were included in this study for comparison. Cumulatively, the two strategies - the double gD retargeting and the gB-gD combination retargeting - result in recombinants which replicate at comparable yields. These studies will help move the field of retargeted oncolytic HSVs to the translational phase.

MATERIALS AND METHODS

Cells and viruses. The J cells (negative for HSV receptors) and their derivatives which transgenically express HER2, nectin1 or HVEM were described (20, 56). The Vero-GCN4R cells were derived from Vero cell (ATCC CCL-81) as described (32). Wt-Vero cells were derived from ATCC. The above cells were grown in DMEM (#31600-083, Gibco Laboratories) supplemented with 5% fetal bovine serum (FBS) (#10270-106 - E.U.-approved, South America origin, Gibco Laboratories). The SK-OV-3 cells were purchased from ATCC and cultured as recommended by ATCC, grown in RPMI 1640-Glutamax (#61870010, Gibco Laboratories) supplemented with 10% heat inactivated fetal bovine serum. hHER2-LLC-1 are the Lewis lung murine carcinoma 1 (LLC-1) cells purchased from ATCC and made transgenic for human HER2. This transgenic cell line will be described elsewhere in details under different co-authorship (37). The recombinant viruses R-LM5, R-LM113 were described (22).

Engineering of HSV recombinants expressing genetically modified gBs. First, we engineered R-313 by insertion of the sequence encoding the GCN4 peptide between aa 43 and 44 of immature gB (corresponding to aa 13 and 14 of mature gB after cleavage of the signal sequence which encompasses aa 1-30). The starting genome was the BAC LM113, which carries scFv-HER2 in place of aa 6 to 38 of gD, LOX-P-bracketed pBeloBAC11 and eGFP sequences inserted between U_L3 and U_L4 of HSV-1 genome (22). The engineering was performed by galK recombineering (57). The GalK cassette with homology arms to gB was amplified by means of primers gB43GalKfor and gB43GalKrev (Table 2) using pgalK as template. This cassette was electroporated in SW102 bacteria carrying the BAC LM113. The recombinant clones carrying the galK cassette were selected as described (22), and screened by colony PCR by means of oligonucleotides galK_129_f and galK_417_r (Table 3). Next, the GCN4 peptide cassette with the downstream and upstream Ser-Gly linkers, bracketed by homology arms to gB was generated through the annealing and extension of oligonucleotides GCN4gB_43_44_fB and GCN4gB_43_44_rB (Table 2), which

317 introduce a silent BamHI restriction site, to enable the screening of colonies. The recombinant
318 clones were screened for the presence of GCN4 peptide by colony PCR with primers gB_ext_for
319 and gB_431_rev (Table 3). R-315 carries the insertion of GCN4 peptide between aa 81 and 82 of
320 HSV gB in the HSV recombinant already expressing a scFv-HER2 in the deletion of aa 6-38 in gD.
321 R-317 carries the insertion of GCN4 peptide between aa 76 and 77 of HSV gB in the HSV
322 recombinant already expressing a scFv-HER2 in the deletion of aa 6-38 in gD. R-319 carries the
323 insertion of GCN4 peptide between aa 95 and 96 of HSV gB in the HSV recombinant already
324 expressing a scFv-HER2 in the deletion of aa 6-38 in gD. R-315, R-317, R-319 were engineered as
325 detailed above for R-313, by means of oligonucleotides reported in Table 2, and screened by PCR
326 by means of oligonucleotides reported in Table 3. R-321 was engineered by reintroduction of aa 6-
327 29 and 31-37 of gD in the HSV recombinant R-313, which carries a scFv-HER2 in the deletion of
328 aa 6-38 in gD and GCN4 peptide between aa 43 and 44 in gB. First, the galK cassette was amplified
329 by means of primers gD5_galK_f
330 TTGTCGTCATAGTGGGCCTCCATGGGGTCCGCGGCAAATATGCCTTGGCGCCTGTTGAC
331 AATTAATCATCGGCA and scFv_galK_rev
332 GAGGCGGACAGGGAGCTCGGGGACTGGGTCATCTGGATATCGGAATTCTCTCAGCACT
333 GTCCTGCTCCTT using pgalK as template. Next, the oligo that comprises aa 6-29 and 31-37 of
334 gD was generated through the annealing and extension of primers gDdel30_38for
335 TTGTCGTCATAGTGGGCCTCCATGGGGTCCGCGGCAAATATGCCTTGGCGGATGCCTCT
336 CTCAAGATGGCCGACCCCAATCGCTTTCGCGGCAAAGACCTTCCGGTCC and
337 gDdel30_38rev
338 GAGGCGGACAGGGAGCTCGGGGACTGGGTCATCTGGATATCGGAATTCTCCACGCGCC
339 GGACCCCCGGAGGGGTCAGCTGGTCCAGGACCGGAAGGTCTTTGCCGCGA.

340 To reconstitute the recombinant viruses R-313, R-315, R-317, R-319 and R-321, 500 ng of
341 recombinant BAC DNA was transfected in SK-OV-3 cells by means of Lipofectamine 2000 (Life
342 Technologies). Virus growth was monitored as green fluorescence. The recombinant viruses that

343 encode for GCN4 peptide, were reconstituted initially in SK-OV-3, frozen/thawed to lyse the SK-
344 OV-3 cells and subsequently grown in Vero-GCN4R cells. Virus stocks were generated in Vero-
345 GCN4R and titrated in Vero-GCN4R, wt-Vero and SK-OV-3 cells. The sequence of gB ORF was
346 verified by sequencing for each recombinant.

347 **Tropism of the recombinant viruses.** The indicated J cell derivatives, wt-Vero, Vero-GCN4R and
348 SK-OV-3 cells were infected with R-313, R-315, R-317, R-319, and R-321 at an input multiplicity
349 of infection of 3 PFU/cell for 90 min at 37°C. The parental R-LM113 virus was included as control.
350 Pictures were taken 24 h after infection by Nikon Eclipse TS100 fluorescence microscope. Where
351 indicated, infection was carried out in the presence of monoclonal antibody (MAb) to HER2
352 (trastuzumab) (28 μg/ml).

353 **Determination of virus growth.** Vero-GCN4R and SK-OV-3 cells were infected at an input
354 multiplicity of infection of 0.1 PFU/cell (as titrated in the correspondent cell line) for 90 min at
355 37°C; unabsorbed virus was inactivated by means of an acidic wash (40 mM citric acid, 10 mM
356 KCl, 135 mM NaCl, pH 3). Replicate cultures were frozen at the indicated times (24 and 48 h) after
357 infection and the progeny was titrated in SK-OV-3. Results are expressed as the mean findings of
358 three independent replicates ± SD.

359 **Cell viability assay.** SK-OV-3 and Vero-GCN4R cells were seeded in 96 well plates 8 x 10^3
360 cells/well, and infected with the indicated viruses or mock-infected for 90 min at 37°C. The input
361 multiplicity of infection (as titrated in the correspondent cell line) was 3 PFU/cell in Vero-GCN4R
362 and 10 PFU/cell in SK-OV-3 cells. AlamarBlue dye (Life Technologies) was added to the culture
363 media (10 μl/well) at the indicated times after infection. The plates were incubated for 4 h at 37°C
364 and read at 560 and 600 nm with GloMax Discover System (Promega) to detect the reduced and
365 oxidized form of alamarBlue dye, respectively. For each time point, cell viability was expressed as
366 the percentage of alamarBlue reduction in infected *versus* uninfected cells, after subtraction of the

367 background value (medium alone). Each point represents the average of at least three triplicate
368 samples ± SD.

369 **Plating efficiency and relative plaque size.** Replicate aliquots of R-313, R-315, R-317, R-
370 319, R-321, R-213, R-LM5 and R-LM113, containing a same amount of virus (50 PFU, as titrated
371 in SK-OV-3 cells), were plated on Vero-GCN4R and SK-OV-3. The infected monolayers were
372 overlaid with medium containing agar and the number of plaques was scored 3 days later. For
373 plaque size determination, 10-fold dilutions R-313, R-315, R-317, R-319, R-321, R-213, R-LM5
374 and R-LM113 were plated onto Vero-GCN4R and SK-OV-3 monolayers. The infected monolayers
375 were overlaid with medium containing agar. Three days later, pictures of 6 plaques were taken at
376 the fluorescence microscope for each virus. Plaque areas (pxE2) were measured with Nis Elements-
377 Imaging Software (Nikon). Each result represents average areas ± SD.

378 **In vivo anti-tumor efficacy.** C57BL6 mice transgenic for and tolerant to hHER2 (B6.Cg-
379 Pds5bTg(Wap-ERBB2)229Wzw/J) received from Jackson Laboratories, were bred in the animal
380 facility of the Department of Veterinary Medical Sciences, University of Bologna. They were
381 implanted with the murine Lewis lung carcinoma 1 (LLC-1) cells made transgenic for hHER2
382 (hHER2-LLC-1), 0.2 x 10E6 cells/mouse (38). Three days later, mice received R-317, or R-LM113
383 and R-87 as control viruses, intratumorally (i.t.), four dosages/mouse at 3-4 days distance, 1 x 10E8
384 PFU/injection. Each treatment group consisted of 5 mice. The tumor size was measured by means
385 of a caliper at the indicated days, as described (23). Animal experiments were performed according
386 to European directive 2010/63/UE, Italian laws 116/92 and 26/2014. The experimental protocols
387 were reviewed and approved by the University of Bologna Animal Care and Use Committee
388 (‘‘Comitato per il Benessere degli Animali”, COBA), and approved by the Italian Ministry of
389 Health, Authorization # 86/2017-PR to Prof. Anna Zaghini.
390

ACKNOWLEDGMENTS

This work was supported by European Research Council (ERC), Advanced Grant number 340060, by Italian Association for Cancer Research, grant number 14535, to G.C.F.

Competing interests. G.C.F. owns shares in Nouscom. B.P. is currently an employee of Nouscom.

FUNDING INFORMATION

EC | European Research Council (ERC) provided funding to Gabriella Campadelli-Fiume under 7th Framework Programme advanced grant number 340060. Italian Association for Cancer Research provided funding to Gabriella Campadelli-Fiume under grant number 14535. The funders had no role in study design, data collection and analysis, decision to publish, or preparation of the manuscript.

REFERENCES

1. **Cattaneo R, Miest T, Shashkova EV, Barry MA.** 2008. Reprogrammed viruses as cancer therapeutics: targeted, armed and shielded. Nat Rev Microbiol **6:**529-540.
2. **Miest TS, Cattaneo R.** 2014. New viruses for cancer therapy: meeting clinical needs. Nat Rev Microbiol **12:**23-34.
3. **Coffin RS.** 2015. From virotherapy to oncolytic immunotherapy: where are we now? Curr Opin Virol **13:**93-100.
4. **Engeland CE, Grossardt C, Veinalde R, Bossow S, Lutz D, Kaufmann JK, Shevchenko I, Umansky V, Nettelbeck DM, Weichert W, Jager D, von Kalle C, Ungerechts G.** 2014. CTLA-4 and PD-L1 checkpoint blockade enhances oncolytic measles virus therapy. Mol Ther **22:**1949-1959.
5. **Mellman I, Coukos G, Dranoff G.** 2011. Cancer immunotherapy comes of age. Nature **480:**480-489.
6. **Keller BA, Bell JC.** 2016. Oncolytic viruses-immunotherapeutics on the rise. J Mol Med (Berl) **94:**979-991.
7. **Campadelli-Fiume G, De Giovanni C, Gatta V, Nanni P, Lollini PL, Menotti L.** 2011. Rethinking herpes simplex virus: the way to oncolytic agents. Rev Med Virol **21:**213-226.
8. **Russell SJ, Peng KW.** 2017. Oncolytic Virotherapy: A Contest between Apples and Oranges. Mol Ther **25:**1107-1116.
9. **Lichty BD, Breitbach CJ, Stojdl DF, Bell JC.** 2014. Going viral with cancer immunotherapy. Nat Rev Cancer **14:**559-567.
10. **Cassady KA, Haworth KB, Jackson J, Markert JM, Cripe TP.** 2016. To Infection and Beyond: The Multi-Pronged Anti-Cancer Mechanisms of Oncolytic Viruses. Viruses **8**.
11. **Fountzilas C, Patel S, Mahalingam D.** 2017. Review: Oncolytic Virotherapy, updates and future directions. Oncotarget doi:10.18632/oncotarget.18309.
12. **Pol J, Buque A, Aranda F, Bloy N, Cremer I, Eggermont A, Erbs P, Fucikova J, Galon J, Limacher JM, Preville X, Sautes-Fridman C, Spisek R, Zitvogel L, Kroemer G, Galluzzi L.** 2016. Trial Watch-Oncolytic viruses and cancer therapy. Oncoimmunology **5:**e1117740.
13. **Liu BL, Robinson M, Han ZQ, Branston RH, English C, Reay P, McGrath Y, Thomas SK, Thornton M, Bullock P, Love CA, Coffin RS.** 2003. ICP34.5 deleted herpes simplex virus with enhanced oncolytic, immune stimulating, and anti-tumour properties. Gene Ther **10:**292-303.
14. **Andtbacka RH, Kaufman HL, Collichio F, Amatruda T, Senzer N, Chesney J, Delman KA, Spitler LE, Puzanov I, Agarwala SS, Milhem M, Cranmer L, Curti B, Lewis K, Ross M, Guthrie T, Linette GP, Daniels GA, Harrington K, Middleton MR, Miller WH, Jr., Zager JS, Ye Y, Yao B, Li A, Doleman S, VanderWalde A, Gansert J, Coffin RS.** 2015. Talimogene Laherparepvec Improves Durable Response Rate in Patients With Advanced Melanoma. J Clin Oncol doi:10.1200/JCO.2014.58.3377.
15. **Russell SJ, Peng KW, Bell JC.** 2012. Oncolytic virotherapy. Nat Biotechnol **30:**658-670.
16. **Chou J, Kern ER, Whitley RJ, Roizman B.** 1990. Mapping of herpes simplex virus-1 neurovirulence to gamma 134.5, a gene nonessential for growth in culture. Science **250:**1262-1266.
17. **Markert JM, Parker JN, Gillespie GY, Whitley RJ.** 2001. Genetically engineered human herpes simplex virus in the treatment of brain tumours. Herpes **8:**17-22.
18. **Zhou G, Roizman B.** 2006. Construction and properties of a herpes simplex virus 1 designed to enter cells solely via the IL-13alpha2 receptor. Proc Natl Acad Sci U S A **103:**5508-5513.

19. **Uchida H, Chan J, Goins WF, Grandi P, Kumagai I, Cohen JB, Glorioso JC.** 2010. A double mutation in glycoprotein gB compensates for ineffective gD-dependent initiation of herpes simplex virus type 1 infection. J Virol **84:**12200-12209.
20. **Menotti L, Cerretani A, Campadelli-Fiume G.** 2006. A herpes simplex virus recombinant that exhibits a single-chain antibody to HER2/neu enters cells through the mammary tumor receptor, independently of the gD receptors. J Virol **80:**5531-5539.
21. **Uchida H, Hamada H, Nakano K, Kwon H, Tahara H, Cohen JB, Glorioso JC.** 2017. Oncolytic Herpes Simplex Virus Vectors Fully Retargeted to Tumor-Associated Antigens. Curr Cancer Drug Targets doi:10.2174/1568009617666170206105855.
22. **Menotti L, Cerretani A, Hengel H, Campadelli-Fiume G.** 2008. Construction of a fully retargeted herpes simplex virus 1 recombinant capable of entering cells solely via human epidermal growth factor receptor 2. J Virol **20:**10153-10161.
23. **Menotti L, Nicoletti G, Gatta V, Croci S, Landuzzi L, De Giovanni C, Nanni P, Lollini PL, Campadelli-Fiume G.** 2009. Inhibition of human tumor growth in mice by an oncolytic herpes simplex virus designed to target solely HER-2-positive cells. Proc Natl Acad Sci USA **106:**9039-9044.
24. **Nanni P, Gatta V, Menotti L, De Giovanni C, Ianzano M, Palladini A, Grosso V, Dall'ora M, Croci S, Nicoletti G, Landuzzi L, Iezzi M, Campadelli-Fiume G, Lollini PL.** 2013. Preclinical Therapy of Disseminated HER-2(+) Ovarian and Breast Carcinomas with a HER-2-Retargeted Oncolytic Herpesvirus. PLoS Pathog **9:**e1003155.
25. **Leoni V, Gatta V, Palladini A, Nicoletti G, Ranieri D, Dall'Ora M, Grosso V, Rossi M, Alviano F, Bonsi L, Nanni P, Lollini PL, Campadelli-Fiume G.** 2015. Systemic delivery of HER2-retargeted oncolytic-HSV by mesenchymal stromal cells protects from lung and brain metastases. Oncotarget.
26. **Gambini E, Reisoli E, Appolloni I, Gatta V, Campadelli-Fiume G, Menotti L, Malatesta P.** 2012. Replication-competent herpes simplex virus retargeted to HER2 as therapy for high-grade glioma. Mol Ther **20:**994-1001.
27. **Gatta V, Petrovic B, Campadelli-Fiume G.** 2015. The Engineering of a Novel Ligand in gH Confers to HSV an Expanded Tropism Independent of gD Activation by Its Receptors. PLoS Pathog **11:**e1004907.
28. **Carter P, Presta L, Gorman CM, Ridgway JB, Henner D, Wong WL, Rowland AM, Kotts C, Carver ME, Shepard HM.** 1992. Humanization of an anti-p185HER2 antibody for human cancer therapy. Proc Natl Acad Sci U S A **89:**4285-4289.
29. **Ross JS, Fletcher JA, Linette GP, Stec J, Clark E, Ayers M, Symmans WF, Pusztai L, Bloom KJ.** 2003. The Her-2/neu gene and protein in breast cancer 2003: biomarker and target of therapy. Oncologist **8:**307-325.
30. **Gu G, Dustin D, Fuqua SA.** 2016. Targeted therapy for breast cancer and molecular mechanisms of resistance to treatment. Curr Opin Pharmacol **31:**97-103.
31. **Kubetzko S, Balic E, Waibel R, Zangemeister-Wittke U, Pluckthun A.** 2006. PEGylation and multimerization of the anti-p185HER-2 single chain Fv fragment 4D5: effects on tumor targeting. J Biol Chem **281:**35186-35201.
32. **Leoni V, Gatta V, Casiraghi C, Nicosia A, Petrovic B, Campadelli-Fiume G.** 2017. A Strategy for Cultivation of Retargeted Oncolytic Herpes Simplex Viruses in Non-cancer Cells. J Virol **91**.
33. **Zahnd C, Spinelli S, Luginbuhl B, Amstutz P, Cambillau C, Pluckthun A.** 2004. Directed in vitro evolution and crystallographic analysis of a peptide-binding single chain antibody fragment (scFv) with low picomolar affinity. J Biol Chem **279:**18870-18877.

34. **Petrovic B, Gianni T, Gatta V, Campadelli-Fiume G.** 2017. Insertion of a ligand to HER2 in gB retargets HSV tropism and obviates the need for activation of the other entry glycoproteins. PLoS Pathog **13:**e1006352.
35. **Nakamura T, Peng KW, Harvey M, Greiner S, Lorimer IA, James CD, Russell SJ.** 2005. Rescue and propagation of fully retargeted oncolytic measles viruses. Nat Biotechnol **23:**209-214.
36. **Cocchi F, Menotti L, Mirandola P, Lopez M, Campadelli-Fiume G.** 1998. The ectodomain of a novel member of the immunoglobulin subfamily related to the poliovirus receptor has the attributes of a bona fide receptor for herpes simplex virus types 1 and 2 in human cells. J Virol **72:**9992-10002.
37. **Leoni V, Petrovic B, Gatta V, Gianni T, Campadelli-Fiume G.** 2017. The simultaneous insertion of two ligands in gD for the cultivation of oncolytic HSVs in non-cancer cells and the retargeting to cancer receptors journal of virology **Submitted**.
38. **Leoni V, Gatta V, Casiraghi C, Vannini A, Zaghini A, Rambaldi J, Barboni C, Lollini P-L, Nanni P, Campadelli-Fiume G.** 2017. A fully virulent HER2-retargeted oncolytic HSV armed with IL12 exerts potent antitumor activity towards distal untreated tumors. Manuscript in preparation
39. **Navarro D, Qadri I, Pereira L.** 1991. A mutation in the ectodomain of herpes simplex virus 1 glycoprotein B causes defective processing and retention in the endoplasmic reticulum. Virology **184:**253-264.
40. **Lee SK, Compton T, Longnecker R.** 1997. Failure to complement infectivity of EBV and HSV-1 glycoprotein B (gB) deletion mutants with gBs from different human herpesvirus subfamilies. Virology **237:**170-181.
41. **Heldwein EE, Lou H, Bender FC, Cohen GH, Eisenberg RJ, Harrison SC.** 2006. Crystal structure of glycoprotein B from herpes simplex virus 1. Science **313:**217-220.
42. **Fan Q, Lin E, Satoh T, Arase H, Spear PG.** 2009. Differential effects on cell fusion activity of mutations in herpes simplex virus 1 glycoprotein B (gB) dependent on whether a gD receptor or a gB receptor is overexpressed. J Virol **83:**7384-7390.
43. **Avitabile E, Forghieri C, Campadelli-Fiume G.** 2009. Cross talk among the glycoproteins involved in herpes simplex virus entry and fusion: the interaction between gB and gH/gL does not necessarily require gD. J Virol **83:**10752-10760.
44. **Potel C, Kaelin K, Gautier I, Lebon P, Coppey J, Rozenberg F.** 2002. Incorporation of green fluorescent protein into the essential envelope glycoprotein B of herpes simplex virus type 1. J Virol Methods **105:**13-23.
45. **Gallagher JR, Atanasiu D, Saw WT, Paradisgarten MJ, Whitbeck JC, Eisenberg RJ, Cohen GH.** 2014. Functional fluorescent protein insertions in herpes simplex virus gB report on gB conformation before and after execution of membrane fusion. PLoS Pathog **10:**e1004373.
46. **Bender FC, Samanta M, Heldwein EE, de Leon MP, Bilman E, Lou H, Whitbeck JC, Eisenberg RJ, Cohen GH.** 2007. Antigenic and mutational analyses of herpes simplex virus glycoprotein B reveal four functional regions. J Virol **81:**3827-3841.
47. **Atanasiu D, Cairns TM, Whitbeck JC, Saw WT, Rao S, Eisenberg RJ, Cohen GH.** 2013. Regulation of herpes simplex virus gB-induced cell-cell fusion by mutant forms of gH/gL in the absence of gD and cellular receptors. MBio **4**.
48. **Lin E, Spear PG.** 2007. Random linker-insertion mutagenesis to identify functional domains of herpes simplex virus type 1 glycoprotein B. Proc Natl Acad Sci U S A **104:**13140-13145.
49. **Uchida H, Chan J, Shrivastava I, Reinhart B, Grandi P, Glorioso JC, Cohen JB.** 2013. Novel mutations in gB and gH circumvent the requirement for known gD Receptors in herpes simplex virus 1 entry and cell-to-cell spread. J Virol **87:**1430-1442.

50. **Hutzen B, Chen CY, Wang PY, Sprague L, Swain HM, Love J, Conner J, Boon L, Cripe TP.** 2017. TGF-beta Inhibition Improves Oncolytic Herpes Viroimmunotherapy in Murine Models of Rhabdomyosarcoma. Mol Ther Oncolytics **7:**17-26.
51. **Moesta AK, Cooke K, Piasecki J, Mitchell P, Rottman JB, Fitzgerald K, Zhan J, Yang B, Le T, Belmontes B, Ikotun OF, Merriam K, Glaus C, Ganley K, Cordover DH, Boden AM, Ponce R, Beers C, Beltran PJ.** 2017. Local Delivery of OncoVEXmGM-CSF Generates Systemic Antitumor Immune Responses Enhanced by Cytotoxic T-Lymphocyte-Associated Protein Blockade. Clin Cancer Res **23:**6190-6202.
52. **Zhou G, Roizman B.** 2007. Separation of receptor binding and pro-fusogenic domains of glycoprotein D of herpes simplex virus 1 into distinct interacting proteins. Proc Natl Acad Sci U S A **104:**4142-4146.
53. **Di Giovine P, Settembre EC, Bhargava AK, Luftig MA, Lou H, Cohen GH, Eisenberg RJ, Krummenacher C, Carfi A.** 2011. Structure of herpes simplex virus glycoprotein d bound to the human receptor nectin-1. PLoS Pathog **7:**e1002277.
54. **Carfi A, Willis SH, Whitbeck JC, Krummenacher C, Cohen GH, Eisenberg RJ, Wiley DC.** 2001. Herpes simplex virus glycoprotein D bound to the human receptor HveA. Mol Cell **8:**169-179.
55. **Connolly SA, Landsburg DJ, Carfi A, Whitbeck CJ, Zuo Y, Wiley DC, Cohen GH, Eisenberg RJ.** 2005. Potential nectin-1 binding site on herpes simplex virus glycoportein D. J Virol **79:**1282-1295.
56. **Cocchi F, Lopez M, Menotti L, Aoubala M, Dubreuil P, Campadelli-Fiume G.** 1998. The V domain of herpesvirus Ig-like receptor (HIgR) contains a major functional region in herpes simplex virus-1 entry into cells and interacts physically with the viral glycoprotein D. Proc Natl Acad Sci U S A **95:**15700-15705.
57. **Warming S, Costantino N, Court DL, Jenkins NA, Copeland NG.** 2005. Simple and highly efficient BAC recombineering using galK selection. Nucleic Acids Res **33:**e36.

FIGURE LEGENDS

Fig. 1. Genome arrangement of recombinants generated in this study. (A) Prototypic genome arrangement of recombinants. Each recombinant carries the BAC sequence and the α27-promoter driven EGFP (enhanced green fluorescence protein), bracketed by LoxP sites, cloned in the UL3 and UL4 intergenic region and the scFv to HER2 in appropriate sites of gD as detailed below. The Unique Long (UL) and Unique Short (US) portions of the genome, bracketed by terminal (TR) and internal repeats (IR), along with the location of gB and gH genes are shown. (B) Specific genotypic modifications of gB and gD genes in each recombinant. (C) Specific genotypic modifications in the gH and gD genes of each recombinant.

Fig. 2. Tropism of R-313, R-315, R-317, R-319, R-321 recombinants, and, for comparison, of R-LM113 in the indicated cells lines. (A-F) The indicated cells were infected with R-313 (A), R-315 (B), R-317 (C), R-319 (D), R-321 (F) and for comparison, R-LM113 (E) at an MOI of 3 PFU/cell and monitored for EGFP expression by fluorescence microscopy 24 h post infection. J-cells express no receptor for wt HSV; J-HER2, J-nectin1, and J-HVEM express the indicated receptor. Infection was carried out in the absence of antibodies (no Ab), or in the presence of the humanized anti-HER2 monoclonal antibody trastuzumab at a concentration of 28 μg/ml. The level, brightness and contrast of each panel were adjusted as follow. R-313 a,b,e +35 +50 +100; c,g +35 0 +100; d,h,i,j +35 0 0; f +0 +95 +95; k +35 +75 +100. R-315 a,b,e,f +35 +50 +100; c +35 0 +100; d,h,i,j,k +35 0 0; g +35 0 +100. R-317 a,b,e,f +35 +50 +100; c +35 0 +100; d,h,i,j,k +35 0 0; g +35 0 +100. R-319 a,b,e,f +35 +50 +100; c +35 0 +100; d,h,i,j,k +35 0 0; g +35 0 +100. R-LM113 a,b +75 +50 +100; c +35 0 +180; d,i,j,k +35 0 0; e,f +35 +50 +100; g +35 0 +100; h +35 -150 0. R-321 a,b,e,f +35 +50 +100; c +35 0 +100; d,h,i,j,k +35 0 0; g +35 0 +100.

Fig. 3. Yield of R-313, R-315, R-317, R-319, R-321 recombinants, and of R-LM5, R-LM113, R-213 and R-87 for comparison. (A, B) SK-OV-3 (A) and Vero-GCN4R (B) cells were infected with

the indicated virus recombinants at 0.1 PFU/cell. Progeny virus was titrated in SK-OV-3 cells at 24 or 48 h after infection. Results represent the average of triplicates, ± SD.

Fig. 4. Plating efficiency and relative plaque size of the indicated recombinants in Vero-GCN4R, and SK-OV-3. (A) A typical plaque is shown for each recombinant in the indicated cells. (B) Average plaque size of the indicated recombinants in Vero-GCN4R and SK-OV-3. Six pictures were taken for each recombinant. Plaque areas were measured by means of Nis Elements-Imaging software (Nikon). (C) Replicate aliquots of recombinants were plated in SK-OV-3 and Vero-GCN4R cells. Plaques were scored three days later. The relative number of plaques formed by each virus in the indicated cell line is reported as percentage of the number of plaques formed in SK-OV-3 cells. Results represent the average of triplicates, ± SD. The level, brightness and contrast of the panel were adjusted as follow: +30 +80 +30. The level, brightness and contrast of R-213 pictures were adjusted as follow: 0 +100 +30.

Fig. 5. Killing ability of the indicated recombinants for SK-OV-3 and Vero-GCN4R cells. (A, B) SK-OV-3 (A) or Vero-GCN4R (B) cells were infected with the indicated recombinants, or with R-LM5 and R-LM113 as controls, at 3 PFU/cell (Vero-GCN4R) and 10 PFU/cell (SK-OV-3). Cell viability was quantified by alamarBlue assay at the indicated days after infection. Results represent a typical experiment; each sample is the average of triplicate assay ± SD.

Fig. 6. Antitumor activity of R-317. (A-C) Groups of 5 mice from the hHER2-transgenic C56BL6 strain were implanted with hHER2-LLC-1 cells in the left flank. Starting 3 d later, mice received four intratumoral treatments at 3-4 d distance with R-317, and with R-LM113 and R-87 as controls, 1 x 10E8 PFU/treatment. Tumor volumes and the number of tumor free animals for each treatment group are shown. (D) Distribution of the tumor size at 28 d after the initial treatment. This experiment is the same as that shown in Fig. 7 of the accompanying paper (37).

634 **Table 1. Major genotypic and phenotypic properties of recombinants described in this study**

Recombinant	GCN4 position in gB	scFv-HER2 position in gD	GCN4 position in gH	Retargeting to HER2	Detargeting from nectin1/HVEM	Ref
R-313	43-44	Δ6-38	None	+	+	This paper
R-315	81-82	Δ6-38	None	+	+	This paper
R-317	76-77	Δ6-38	None	+	+	This paper
R-319	95-96	Δ6-38	None	+	+	This paper
R-321	43-44	Δ30, 38	None	+	+	This paper
R-87	None	Δ35-39 plus GCN4 between aa 24 and 25	None	+	+	(37)
R-213	None	Δ6-38	23-24	+	+	(32)
R-LM113	None	Δ6-38	None	+	+	(22)
R-LM5	None	No scFv, no deletion	None	-	-	(22)

635
636
637
638 **Table 2. Oligonucleotides employed to engineer the indicated recombinant genomes**
639

Recombinant	GalK recombination		GCN4 recombination	
R-313	gB43GalKfor	GGTGGCGTCGGCGGCTCCGAGTTCCCCCGGCACGCCTGGGGTCGCGGCCGCGCCTGTTGACAATTAATCATCGGCA	GCN4gB_43_44_fB	GGTGGCGTCGGCGGCTCCGAGTTCCCCCGGCACGCCTGGGGTCGCGGCCGCGGGATCCAAGAACTACCACCTGGAGAACGAGGTGGCCAGACTGAAGAAGCTGGTGGGCAGC
	gB43GalKrev	GGCCAGGGGCGGGCGGCGCCGGAGTGGCAGGTCCCCCGTTCGCCGCCTGGGTTCAGCACTGTCCTGCTCCTT	GCN4gB_43_44_rB	GGCCAGGGGCGGGCGGCGCCGGAGTGGCAGGTCCCCCGTTCGCCGCCTGGGTGCTGCCCACCAGCTTCTTCAGTCTGGCCACCTCGTTCTCCAGGTGGTAGTTCTTGGATCC
R-315	gB81fGALK	CGGGGGACACGAAACCGAAGAAGAACAAAAAACCGAAAAACCCACCGCCGCCGCCTGTTGACAATTAATCATCGGCA	gB_81_GCN4_for	CGGGGGACACGAAACCGAAGAAGAACAAAAAACCGAAAAACCCACCGCCGCCGGGATCCAAGAACTACCACCTGGAGAACGAGGTGGCCAGACTG

				AAGAAGCTGGTGG GCAGC
	gB81GALKrev	CGCAGGGTGGC GTGGCCCGCGG CGACGGTCGCG TTGTCGCCGGC GGGGCGTCAGC ACTGTCCTGCTC CTT	gB_81_GCN4_rev	CGCAGGGTGGCGTG GCCCGCGGCGACGG TCGCGTTGTCGCCG GCGGGGCGGCTGCC CACCAGCTTCTTCA GTCTGGCCACCTCG TTCTCCAGGTGGTA GTTCTTGGATCC
R-317	gB_76_galK_for	GGCCCCGCCCC AACGGGGGACA CGAAACCGAAG AAGAACAAAAA ACCGAAACCTG TTGACAATTAA TCATCGGCA	gB_76_GCN4_for	GGCCCCGCCCCAAC GGGGGACACGAAA CCGAAGAAGAACA AAAAACCGAAAGG ATCCAAGAACTACC ACCTGGAGAACGA GGTGGCCAGACTGA AGAAGCTGGTGGGC AGC
	gB_76_galK_rev	CCCGCGGCGAC GGTCGCGTTGT CGCCGGCGGGG CGCGGCGGCGG TGGGTTTCAGC ACTGTCCTGCTC CTT	gB_76_GCN4_rev	CCCGCGGCGACGGT CGCGTTGTCGCCGG CGGGGCGCGGCGG CGGTGGGTTGCTGC CCACCAGCTTCTTC AGTCTGGCCACCTC GTTCTCCAGGTGGT AGTTCTTGGATCC
R-319	gB_95_galK_for	CGCCGCCGCGC CCCGCCGGCGA CAACGCGACCG TCGCCGCGGGC CACGCCCCTGTT GACAATTAATC ATCGGCA	gB_95_GCN4_for	CGCCGCCGCGCCCC GCCGGCGACAACGC GACCGTCGCCGCGG GCCACGCCGGATCC AAGAACTACCACCT GGAGAACGAGGTG GCCAGACTGAAGA AGCTGGTGGGCAGC
	gB_95_galK_rev	GTTTGCATCGGT GTTCTCCGCCTT GATGTCCCGCA GGTGCTCGCGC AGGGTTCAGCA CTGTCCTGCTCC TT	gB_95_GCN4_rev	GTTTGCATCGGTGT TCTCCGCCTTGATG TCCCGCAGGTGCTC GCGCAGGGTGCTGC CCACCAGCTTCTTC AGTCTGGCCACCTC GTTCTCCAGGTGGT AGTTCTTGGATCC

Table 3. Oligonucleotides employed for the diagnostic PCR of the indicated recombinant genomes

Recombinant	GalK recombination		GCN4 recombination	
R-313, R-315, R-317 and R-319	galK_129_f	ACAATCTCTGTTTG CCAACGCATTTGG	gB_ext_for	GAGCGCCCCCGACGGC TGTATCG
	galK_417_r	CATTGCCGCTGATC ACCATGTCCACGC	gB_431_rev	TTGAAGACCACCGCGA TGCCCT

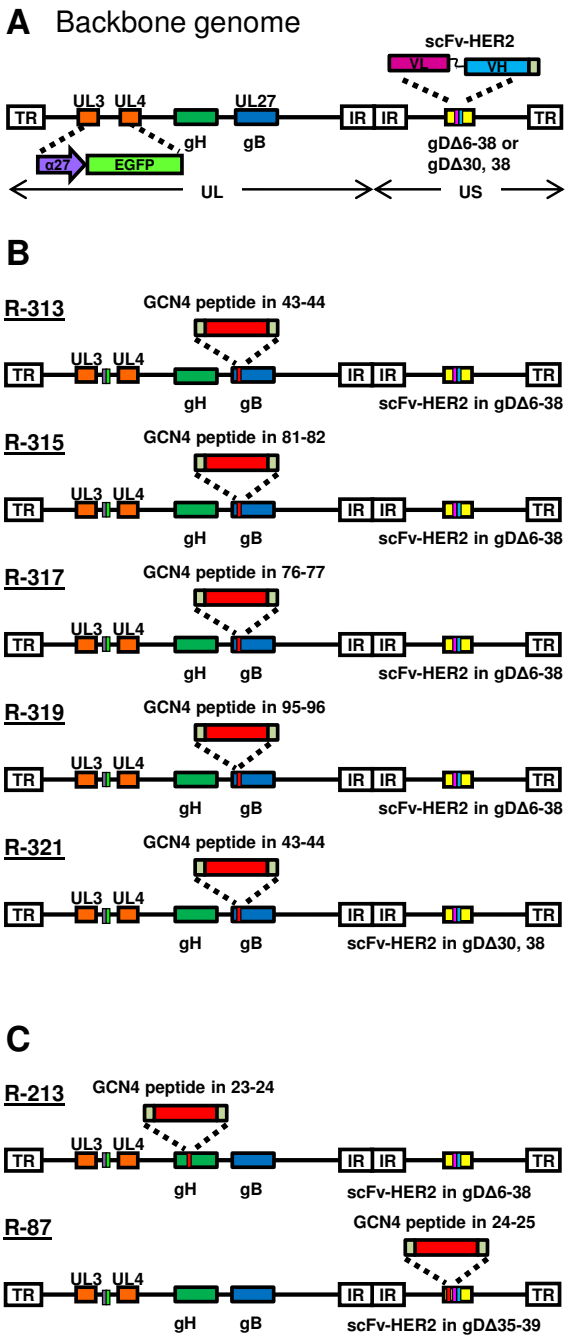

Figure 1

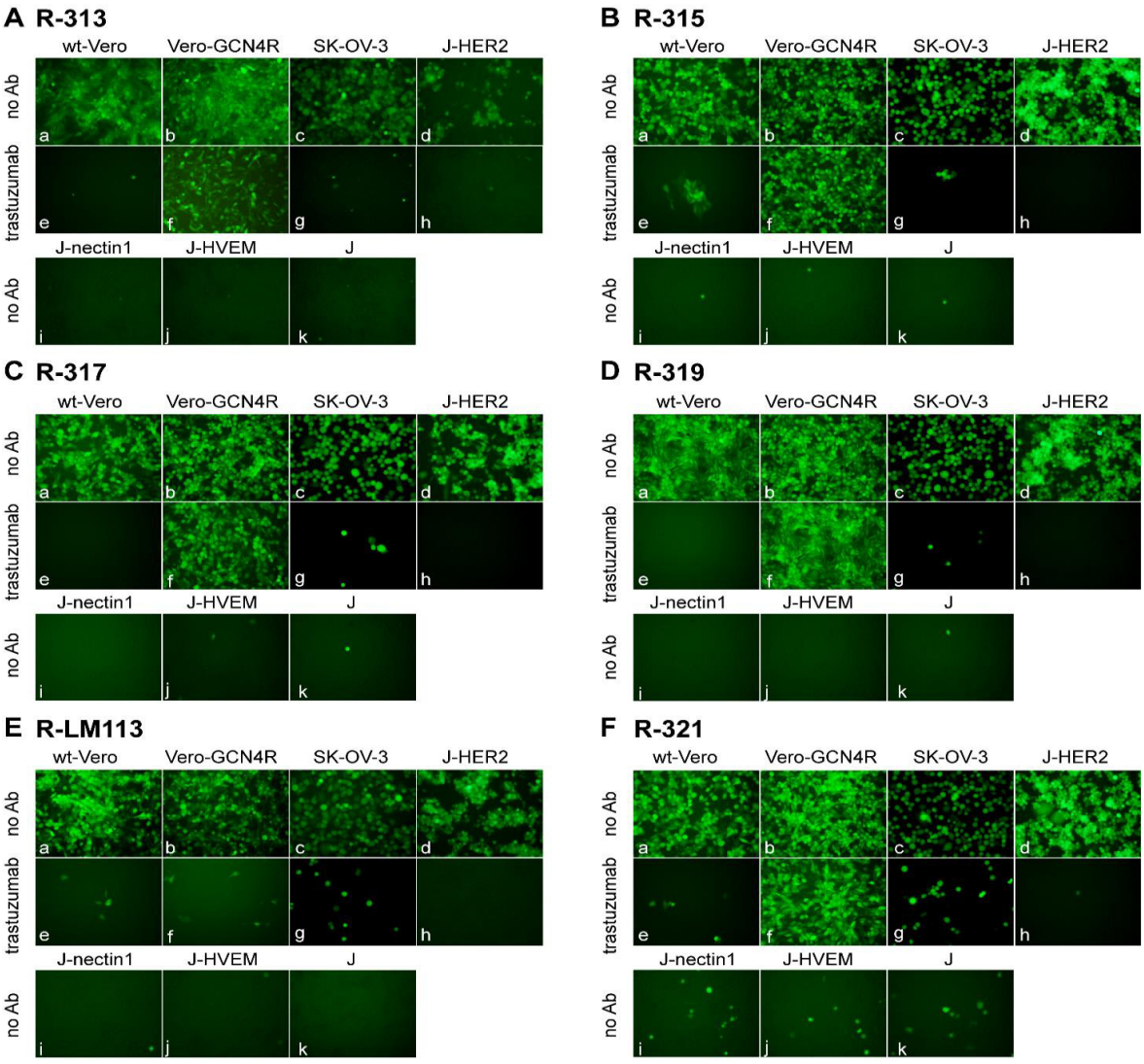

Figure 2

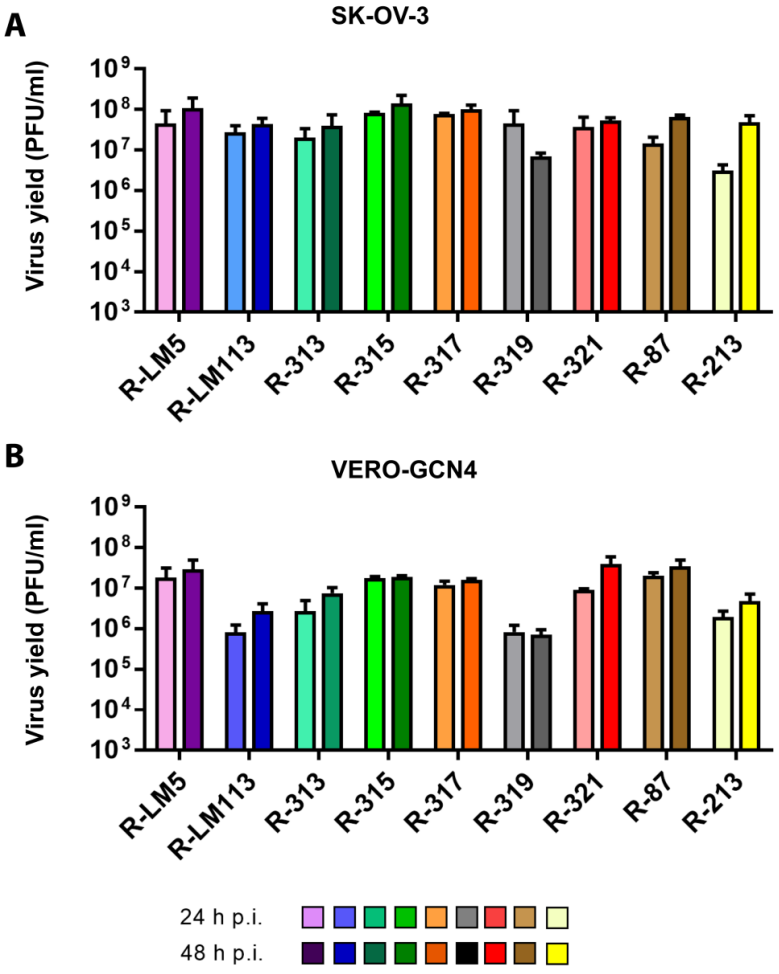

Figure 3

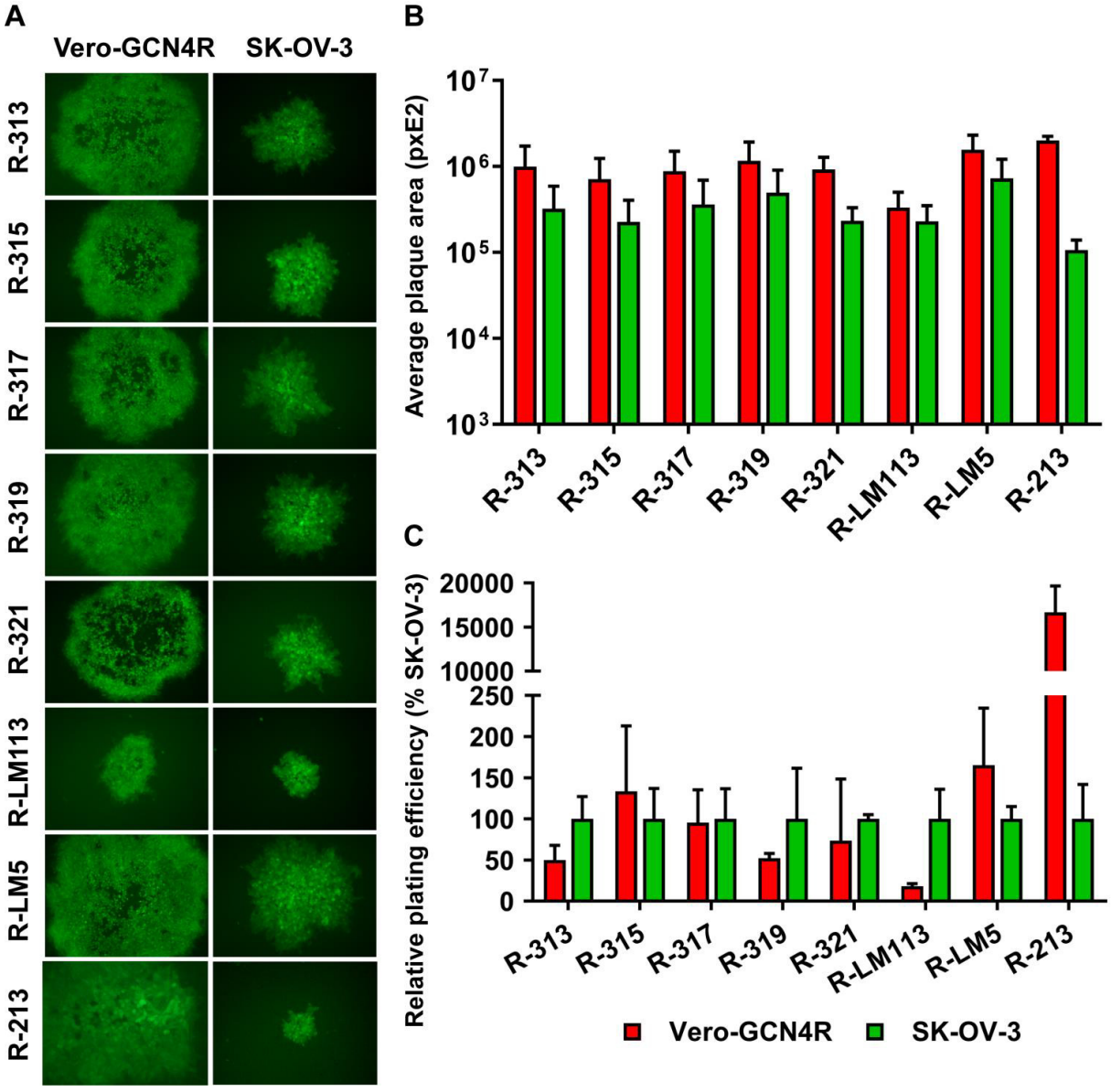

Figure 4

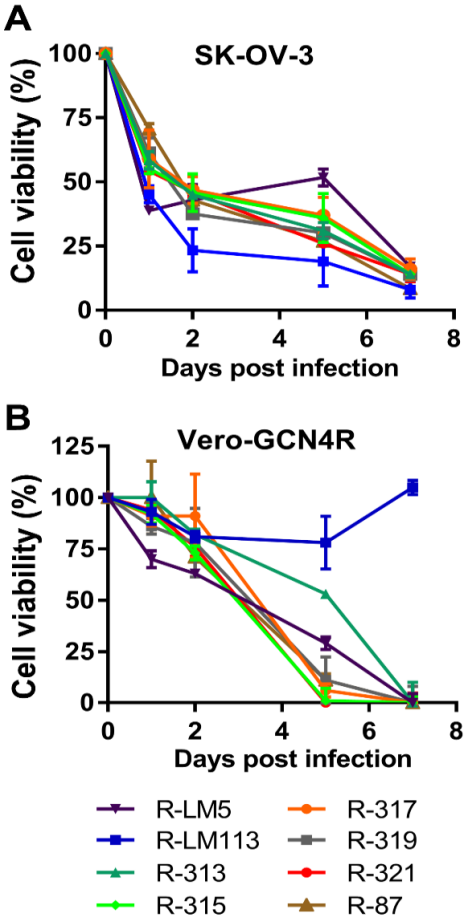

Figure 5

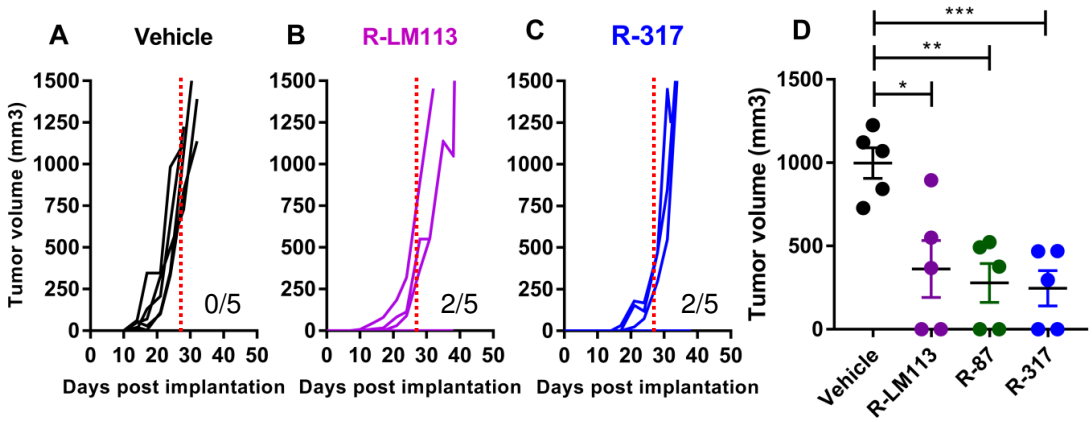

Figure 6